6. M. Abramowitz and I. A. Stegun (eds.), Handbook of Mathematical Functions, U.S. Govt. Printing Office, Washington, DC (1964).
7. M. Reed and B. Simon (eds.), Methods of Modern Mathematical Physics, Vol. 1: Functional Analysis, Academic Press, New York (1972).
8. L. V. Kantorovich and G. P. Akilov, Functional Analysis [in Russian], Nauka, Moscow (1977).
9. E. I. Nefedov and A. N. Sivov, Electrodynamics of Periodic Structures [in Russian], Nauka, Moscow (1977).
10. D. N. Gorelov, V. B. Kurzin, and V. É. Saren, Atlas of Transient Aerodynamic Characteristics of Blade-Profile Cascades [in Russian], Nauka, Novosibirsk (1974).

LARGE-PARTICLE STUDY OF THE FLOW AROUND WORKING BLADES IN A STEAM TURBINE

Yu. M. Davydov, V. D. Kulikov, and E. V. Maiorskii

UDC 621.165-226.1.001.5

High supersonic velocities and a very complicated flow structure occur in the flow around the blade profiles in steam turbines, particularly the peripheral sections of the latter stages in low-pressure cylinders. It is therefore impossible to predict details of the flow. Measurements on such blades are complicated and expensive. It is therefore desirable to use numerical simulation in a preliminary analysis of the flow structure.

For example, calculations have been performed by Godunov's method [1] on the working and nozzle profiles [2-4].

The large-particle method is now widely used [5, 6], particularly for many aspects of gas dynamics, including the calculation of internal flows [7]. Here we demonstrate its use in numerical examination of a new class of topics: calculating the flow around turbine blade profiles.

Figure 1 shows one of the sets of blades (form I). The calculations were performed for an inlet angle $\beta_1 = 163°$, an angle of attack $i = \beta_1 - \beta_0 = \pm 4°13'$, and a relative pitch of $\bar{t} = t/b = 1.02$.

We considered typical modes of flow around the blades, in which subsonic velocities $M_1 \approx 0.5$ occurred at the inlet and supersonic ones $M_2 \approx 1.9$.

The working region ACDE (Fig. 1) of rectangular shape is split up into several zones differing in the sizes of the rectangular cells in the immobile net. The smallest cells lie in the regions of the inlet edges F and the outlet ones K, where the curvature is maximal. Here the profile contour was calculated with the necessary accuracy.

The total number of cells varied from 4000 to 6000. The calculations were performed with an ES-1040 computer (OS operating system) on a FORTRAN program; the run time for one model was not more than 6 h.

The boundary conditions were specified as follows. At the boundaries AC and ED, periodicity conditions applied. The boundary AE (Fig. 1) was taken at a distance t along the normal to the input front (line $a\bar{l}$). Test calculations showed that any further increase in this distance had no effect on the results. The conditions for constancy of the entropy S, total enthalpy J_0, and direction of the velocity vector β_1 were taken at the boundary AE:

$$S = p/\rho^k = \text{const}, \quad J_0 = \frac{k}{k-1}\frac{p}{\rho} + \frac{W^2}{2} = \text{const}, \quad \beta_1 = \text{const},$$

where p, ρ, W, and k are correspondingly pressure, density, velocity, and isentrope parameters. Also we maintained the condition for conservation of the left Riemann invariant in each time layer [8]: $RM = W - 2a(k-1)$, where $a = \sqrt{kp/\rho}$.

Moscow. Translated from Zhurnal Prikladnoi Mekhaniki i Tekhnicheskoi Fiziki, No. 3, pp. 47-50, May-June, 1984. Original article submitted April 6, 1983.

0021-8944/84/2503-0373$08.50

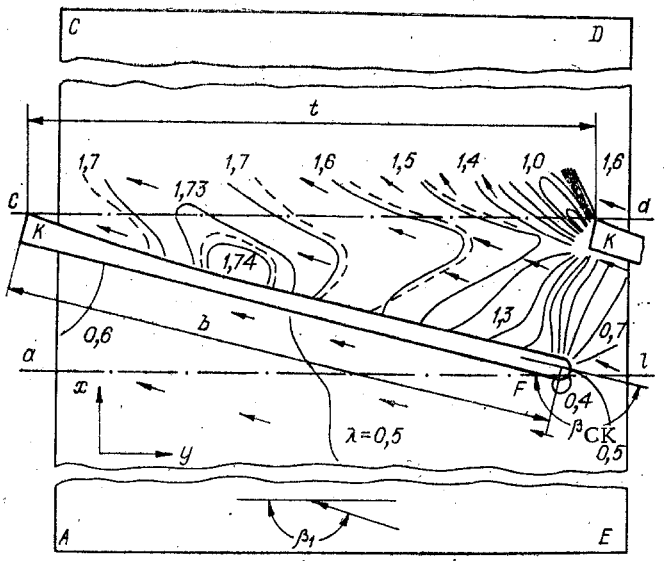

Fig. 1

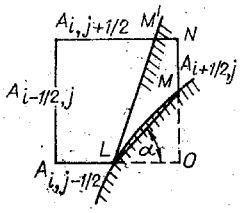

Fig. 2

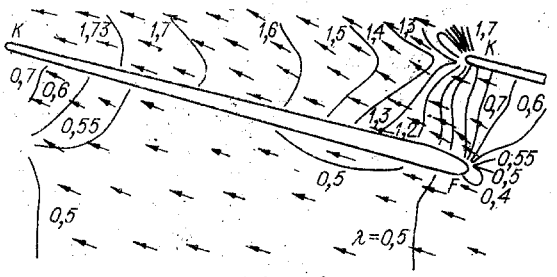

Fig. 3

We examined the boundary conditions along CD for the maximum value of M_2, which showed that the distance along the normal to the front at the exit (line cd) cannot exceed t for an assembly of this type (calculations were performed in the range 0.2 t to 1.5 t). Figure 1 shows the results: the lines $\lambda = W/a_* = \text{const}$ (where a_* is the critical velocity) and the directions of the velocity vectors for the case where the boundary CD lay at distances of 1.0 t (solid lines) and 1.5 t (dashed lines) for constant parameters along boundary CD.

We also examined two ways of specifying the boundary conditions along CD: All the parameters in a fictitious cell layer were taken either as constant (with extension to this layer of the values of β_2 from the adjacent layer) or else only the pressure p_2 was taken as constant while conserving the right Riemann invariant and the entropy. Similar values for the flow parameters were obtained in the numerical calculations, which showed that both methods of specifying the boundary conditions at CD can be used in flow calculations.

The conditions for no flow were specified along the profile contour. The fractional-cell approach [9] was used, as modified for the specific form of the profiles. A feature of these is that the profiles have very small relative thickness, so not all the necessary fictitious cells can be generated within the profile. They therefore would have to be specified outside the physical region, which would cause difficulties in the program. Therefore, the method of specifying the boundary conditions along the profiles ruled out the specification of fictitous cells.

The pressure at the profile within a fractional cell was taken as equal to the pressure at the center of this cell $p_{i,j}$, while the velocity vector was taken as equal to the component of the velocity vector $W_{i,j}$ parallel to the line LM (Fig. 2). The parameters in the fractional cell i, j were determined in the Euler stage by means of the following system of equations:

$$\tilde{u}^n_{i,j} = u^n_{i,j} - \frac{\left[A_{i+1/2,j}p^n_{i+1/2,j} - A_{i-1/2,j}p^n_{i-1/2,j} + (A_{i-1/2,j} - A_{i+1/2,j})\,p^n_{i,j}\right]\Delta t}{\Delta x \max\left(A_{i,j+1/2}, A_{i,j-1/2}\right) f_{i,j}\rho^n_{i,j}}. \qquad (1)$$

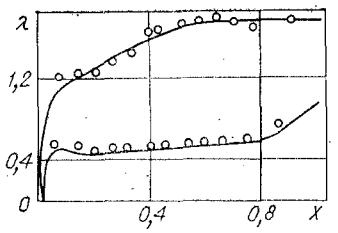

Fig. 4

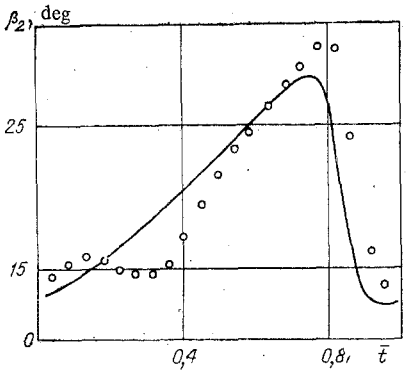

Fig. 5

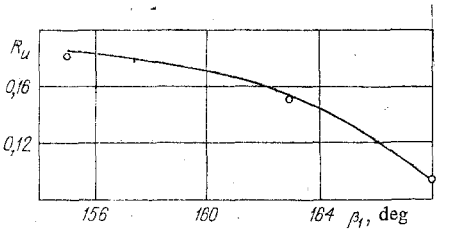

Fig. 6

$$\tilde{v}^n_{i,j} = v^n_{i,j} - \frac{\left[A_{i,j+1/2}p^n_{i,j+1/2} - A_{i,j-1/2}p^n_{i,j-1/2} + (A_{i,j-1/2} - A_{i,j+1/2})\,p^n_{i,j}\right]\Delta t}{\Delta y \max\left(A_{i-1/2,j}\,A_{i+1/2,j}\right) f_{i,j}p^n_{i,j}},$$

$$\tilde{E}^n_{i,j} = E^n_{i,j} - \left[\frac{A_{i+1/2,j}p^n_{i+1/2,j}u^n_{i+1/2,j} - A_{i-1/2,j}p^n_{i-1/2,j}u^n_{i-1/2,j} + (A_{i-1/2,j} - A_{i+1/2,j})\,p^n_{i,j}u}{\Delta x \max\left(A_{i,j-1/2},\,A_{i,j+1/2}\right)} + \right.$$

$$\left. + \frac{A_{i,j+1/2}p^n_{i,j+1/2}v^n_{i,j+1/2} - A_{i,j-1/2}p^n_{i,j-1/2}v^n_{i,j-1/2} + (A_{i,j-1/2} - A_{i,j+1/2})\,p^n_{i,j}v_н}{\Delta y \max\left(A_{i-1/2,j},\,A_{i+1/2,j}\right)}\right]\frac{\Delta t}{f_{i,j}\rho^n_{i,j}},$$

where $A_{i+1/2,j}$, $A_{i-1/2,j}$, $A_{i,j+1/2}$, $A_{i,j-1/2}$ are the parts of the sides of the cells open for liquid flow. If the contour intersects a cell along the LM line, then $A_{i+1/2,j} = 0$. The following formulas give the vertical and horizontal velocity-vector components at the contour:

$$v_1 = (u^n_{i,j}\operatorname{tg}\alpha + v^n_{i,j})/1 - \operatorname{tg}^2\alpha, \quad u_1 = \operatorname{tg}\alpha\,(u^n_{i,j}\operatorname{tg}\alpha + v^n_{i,j})/1 - \operatorname{tg}^2\alpha,$$

where

$$\operatorname{tg}\alpha = \frac{A_{i,j+1/2} - A_{i,j-1/2}}{A_{i-1/2,j} - A_{i+1/2,j}}.$$

System (1) corresponds in structure to a simple finite-difference approximation to the system of equations for whole cells [5, 6]. For example, the expression $A_{i+1/2,j}p^n_{i+1/2,j}$ is the pressure on part of the open side of a fractional cell (NM), while $(A_{i-1/2,j} - A_{i+1/2,j})\,p_{i,j}$ is the pressure on the part of the side of that cell lying within the body. Consequently, the product $A_{i-1/2,j}p_{i-1/2,j}$ corresponds to the pressure on the left open boundary of the cell, while the sum of the products $A_{i+1/2,j}p_{i+1/2,j} + (A_{i-1/2,j} - A_{i+1/2,j})\,p^n_{i,j}$ corresponds to that on the right fractional side (NO) of the cell.

The equations for the Lagrange and final stages are then as in [9].

Figure 3 shows an array of profiles of a different configuration (form II) with $\bar{t} = 0.96$. The flow calculations were performed for the same conditions as I (p, ρ, and W = const at the boundary CD). Then i = −1°09'. Comparison of the results (Fig. 3) with Fig. 1 shows that they are identical in the region of minimum cross section (the throat), while at the same time there is a substantial effect from the shape of the low-pressure side in oblique section on the character of the flow. There are also differences in the flow on the pressure side.

Figures 4 and 5 compare the calculations (solid lines) for case II with experiments performed on a steam-dynamic tube at Moscow Power Institute: Fig. 4 compares the results for $\lambda = f(X)$ on the flow around the profile ($X = x/b$, where x is the distance from the inlet edge along the contour), and Fig. 5 compares the angles for the velocity vector behind the assembly at a distance 0.2b (profile chords) along the normal to the line cd at the length of one step.

This example shows satisfactory agreement between calculation and experiment. Similar satisfactory agreement occurs for other flow conditions in these assemblies. We give for example a comparison for the characteristic of practical importance known as the relative circumferential force $R_u = r_u/[(p_0 - p_2)_b]$ (p_0 is the stagnation pressure ahead of the assembly and p_2 is the pressure behind it) acting on a single profile in case II with a variable inlet angle (Fig. 6). Here again there is satisfactory agreement between theory and experiment. In these calculations, the difference net was fairly coarse, so the fine structure of the flow was not revealed in zones close to the profile edges. This feature does not have any substantial effect on most of the characteristics. The accuracy for details of the flow could be raised by using a computer faster than the ES-1040. This careful analysis confirms that the large-particle method is highly effective in application to the flow in a system of interacting bodies of complicated shape: a turbine blade assembly. This enables one to reduce the number of experiments required considerably in designing new assemblies and upgrading aerodynamic performance.

LITERATURE CITED

1. S. K. Godunov, "A difference method of deriving discontinuous solutions in hydrodynamics," Mat. Sb., 47, Issue 89 (1959).
2. S. K. Godunov (ed.), Numerical Solution of Multidimensional Problems in Gas Dynamics [in Russian], Nauka, Moscow (1976).
3. G. A. Sokolovskii and V. I. Gnesin, Calculation of Mixed Flows in Turbine Assemblies [in Russian], Naukova Dumka, Kiev (1981).
4. L. A. Dorfman, Numerical Methods in the Gas Dynamics of Turbines [in Russian], Énergiya, Leningrad (1974).
5. O. M. Belotserkovskii and Yu. M. Davydov, The Large-Particle Method in Gas Dynamics [in Russian], Nauka, Moscow (1982).
6. Yu. M. Davydov, "The large-particle method," in: Mathematics Encyclopedia, Vol. 3 [in Russian], Sov. Entsiklopediya, Moscow (1982).
7. Yu. M. Davydov, "Calculating some internal gas flows by the large-particle method," Prikl. Mekh., 14, No. 4 (1978).
8. L. D. Landau and E. M. Lifshits, Mechanics of Continuous Media [in Russian], Gostekhizdat, Moscow (1953).
9. Yu. M. Davydov, "Calculating the flow around bodies of arbitrary shape by the large-particle method," Zh. Vysshl. Mat. Mat. Fiz., 11, No. 4 (1971).